Photochemistry and Photobiology, 2006, 82: 398–405

Photochemopreventive Effect of Pomegranate Fruit Extract on UVA-mediated Activation of Cellular Pathways in Normal Human Epidermal Keratinocytes

Deeba N. Syed, Arshi Malik, Naghma Hadi, Sami Sarfaraz, Farrukh Afaq and Hasan Mukhtar*

Department of Dermatology, University of Wisconsin, Madison, WI

Received 23 June 2005; accepted 22 November 2005; published online 29 November 2005 DOI: 10.1562/2005-06-23-RA-589

ABSTRACT

UVA is the major portion (90–99%) of solar radiation reaching the surface of the earth and has been described to lead to formation of benign and malignant tumors. UVA-mediated cellular damage occurs primarily through the release of reactive oxygen species and is responsible for immunosuppression, photodermatoses, photoaging and photocarcinogenesis. Pomegranate fruit extract (PFE) possesses strong antioxidant and anti-inflammatory properties. Our recent studies have shown that PFE treatment of normal human epidermal keratinocytes (NHEK) inhibits UVB-mediated activation of MAPK and NF-κB pathways. Signal transducers and activators of transcription 3 (STAT3), Protein Kinase B/AKT and Map Kinases (MAPKs), which are activated by a variety of factors, modulate cell proliferation, apoptosis and other biological activities. The goal of this study was to determine whether PFE affords protection against UVA-mediated activation of STAT3, AKT and extracellular signal–regulated kinase (ERK1/2). Immunoblot analysis demonstrated that 4 J/cm^2 of UVA exposure to NHEK led to an increase in phosphorylation of STAT3 at Tyr^{705}, AKT at Ser^{473} and ERK1/2. Pretreatment of NHEK with PFE (60–100 μg/mL) for 24 h before exposure to UVA resulted in a dose-dependent inhibition of UVA-mediated phosphorylation of STAT3 at Tyr^{705}, AKT at Ser^{473} and ERK1/2. mTOR, structurally related to PI3K, is involved in the regulation of p70S6K, which in turn phosphorylates the S6 protein of the 40S ribosomal subunit. We found that UVA radiation of NHEK resulted in the phosphorylation of mTOR at Thr^{2448} and p70S6K at Thr^{421}/Ser^{424}. PFE pretreatment resulted in a dose-dependent inhibition in the phosphorylation of mTOR at Thr^{2448} and p70S6K at Thr^{421}/Ser^{424}. Our data further demonstrate that PFE pretreatment of NHEK resulted in significant inhibition of UVA exposure–mediated increases in Ki-67 and PCNA. PFE pretreatment of NHEK was found to increase the cell-cycle arrest induced by UVA in the G1 phase of the cell cycle and the expression of Bax and Bad (proapoptotic proteins), with downregulation of Bcl-X$_L$ expression (antiapoptotic protein). Our data suggest that PFE is an effective agent for ameliorating UVA-mediated damages by modulating cellular pathways and merits further evaluation as a photochemopreventive agent.

INTRODUCTION

UV radiation (UVR) causes many adverse events in human, including erythema, hyperplasia, hyperpigmentation, immunosuppression and photoaging (1,2). UVR from the solar spectrum is divided into different energy levels, ranging from short to long wavelengths. UVA is the major component and extends from 320 to 400 nm, UVB from 280 to 320 nm and UVC from 185 nm to 280 nm. UVA comprises the largest portion (90–99%) of the solar radiation reaching the surface of the earth and has been described to lead to benign and malignant skin cancers (3). It is not absorbed by the ozone layer, unlike UVC, and has a deeper penetration in the skin, increasing the potential risk from UVA exposure. The carcinogenic properties of UVB result from direct damage to DNA. In contrast, UVA-induced effects are thought to be indirect results of oxidative damage caused primarily through the release of singlet oxygen, resulting in genomic alterations varying from point mutations to crude chromosomal dislocations (3–5). Various signal-transduction pathways, transcription factors and changes in gene expression are involved in UV-mediated proliferation, differentiation and apoptosis of skin cells (1,6).

The oxidative damage caused by UV results in inflammation, gene mutation and immunosuppression, all of which are critical components of tumor progression. A number of inflammatory pathways may be induced, further contributing to skin carcinogenesis. Signal transducers and activators of transcription 3 (STAT3), latent cytoplasmic proteins activated via tyrosine phosphorylation in response to UV, cytokines and growth factors regulate the expression of many genes (7–9). STAT3 has been shown to be constitutively activated in a number of human malignancies and abrogation of its function leads to apoptosis or inhibition of cell proliferation in various cell lines (10). AKT protein kinase, activated by growth factors, is primarily involved in cell survival. It has been shown that apoptosis induced by UVA is suppressed by activation of insulin-like growth factors, which in turn activate the PI3K/AKT pathway (11). Extracellular signal–regulated kinases (ERKs) of the superfamily MAPK are involved in regulating cellular functions, such as development, growth, differentiation, proliferation and programmed cell death (*i.e.* apoptosis) (12). It has been reported that PKC-mediated ERK activation by UVA provides a signal for the keratinocytes to escape apoptosis (13). Mammalian target of rapamycin (mTOR) is a serine-threonine kinase involved in the regulation of

*Corresponding author email: hmukhtar@wisc.edu (Hasan Mukhtar)

cell growth through initiation of gene translation. Rapamycin, an mTOR inhibitor, has emerged as an immunosuppressive and antiproliferative drug, and is considered a novel antitumor agent. mTOR has been shown to be required for p70S6K activation and phosphorylation induced by UVA exposure (14). mTOR initiates translation by activating p70S6K, which in turn phosphorylates the S6 protein of the 40S ribosomal subunit (15) directing the cell toward increased production of ribosomal proteins and elongation factors.

Members of the Bcl-2 family of proteins include both antiapoptotic molecules such as Bcl-2 and Bcl-X_L, and proapoptotic molecules such as Bax, Bak, Bid and Bad; crucial regulators of programmed cell death or apoptosis. The majority of human cancers are associated with overexpression of Bcl-2, Bcl-X_L or both. The complex process of apoptosis involves a balance between proapoptotic and antiapoptotic proteins. Studies in the mouse model have shown that short-term UV exposure results in an apoptotic response through induction of the Bax protein, with a concomitant decrease in Bcl-2 proteins (16). Bax (–/–) mice showed a significant increase in tumor incidence when exposed to UV-induced stress in two-step chemical carcinogenesis studies, compared with control mice (17). Bcl-X_L expressed abundantly in the epidermis prevents cell death induced by UV radiation and other mutagens (18) and its overexpression in transgenic mice dramatically increases the rate of conversion of benign tumors to malignant tumors (19).

Development of effective photochemopreventive agents capable of ameliorating the effects of UV-induced damage is an area of ongoing research. One such agent is pomegranate derived from the tree *Punica granatum*, a fruit recognized since antiquity for its healing properties. Recent studies are showing that pomegranate juice has beneficial effects in humans. The antioxidant and antiviral properties of pomegranate juice are noteworthy (20,21). Also documented are its antiproliferative, antiinvasive and proapoptotic actions in cancer cell lines, as well as its antiangiogenic activities, both *in vitro* and *in vivo* (22). We have recently used the mouse skin two-step carcinogenesis protocol (23) to show that pomegranate fruit extract (PFE) is an effective antitumor-promoting agent and inhibits UVB-mediated phosphorylation of MAPK and activation of NF-κB in normal human epidermal keratinocytes (NHEK) (24). In the present study we determined the effect of PFE treatment of NHEK on UVA-induced changes in markers of cell proliferation, such as STAT3, AKT1, ERK1/2, PCNA, Ki-67 and regulators of translational machinery, such as mTOR and its downstream target p70S6K. We also studied the effect of PFE on UVA-mediated modulations in members of the Bcl-2 family of proteins, namely the proapoptotic molecules Bad and Bax and the antiapoptotic molecule Bcl-X_L.

MATERIALS AND METHODS

Materials. ERK1/2 (phospho-p44/42, Thr^{202}/Tyr^{204}), STAT3 (phospho-STAT3, Tyr^{705}), mTOR (phospho-Ser^{2448}) and p70S6 kinase (phospho-Thr^{421}/Ser^{424}) antibodies were purchased from Cell Signaling Technology (Beverly, MA). AKT1 (phospho-Ser^{473}), Bad, Bax and Bcl-X_L antibodies were obtained from Upstate Biotechnology (Lake Placid, NY). PCNA and Ki-67 antibodies were purchased from Santa Cruz Biotechnology (Santa Cruz, CA). Anti-mouse or anti-rabbit secondary antibody horse-radish peroxidase conjugate was obtained from Amersham Life Science Inc. (Arlington Height, IL). The DC Bio-Rad Protein assay kit was purchased from Bio-Rad Laboratories (Hercules, CA). Novex precast Tris-Glycine gels were obtained from Invitrogen (Carlsbad, CA).

Preparation of pomegranate fruit extract. Fresh pomegranate procured from the local supermarket was peeled and its edible portion (seed coat and juice) was squeezed in 70% acetone-30% distilled water (1:20 w/v). The red extract was filtered through filter paper No. 1 (Whatman Limited, England). The filtrate was condensed and freeze-dried. The freeze-dried extract was stored at 4°C to be used for treatment of NHEK. On the basis of matrix-assisted laser desorption ionization time of flight mass spectrometry analysis, PFE was found to contain anthocyanins and hydrolyzable and oligomeric tannins in which two to five glucose units are crosslinked by dehydrodigalloyl units (23).

Cell culture. The NHEK were obtained from Invitrogen Corporation (Carlsbad, CA) and the primary cultures were maintained in keratinocyte-SFM medium (Life Technologies, Grand Island, NY) supplemented with 0.1 m*M* calcium, 0.2% v/v bovine pituitary extract, EGF (10 ng/mL), insulin (5 μg/mL), hydrocortisone (5×10^{-7} *M*), ethanolamine (1×10^{-4} *M*), phosphoethanolamine (1×10^{-4} *M*) and L-glutamine. The cells were maintained at 95% humidity in a 5% CO_2 environment at 37°C. Cells obtained between the third and fifth pass were used in the present study.

Treatment of cells. PFE dissolved in dimethyl sulfoxide (DMSO) was used for the treatment of cells. The final concentration of DMSO used was 0.1% v/v for each treatment. For dose-dependent studies, the cells (70–80% confluent) were treated with PFE (60, 80 and 100 μg/mL) for 24 h in keratinocyte-SFM medium, after which the medium was removed and cells were washed with PBS; fresh PBS was added and these PFE-pretreated cells were irradiated with 4 J cm^{-2} of UVA with a custom-designed research irradiation unit (Daavlin, Bryan, OH) that consists of a fixture mounted on fixed legs. Mounted within the exposure unit are four UVA lamps and the exposure system is controlled using Daavlin Flex Control Integrating Dosimeters. In this system dose units can be calculated in Joules per square centimeter for UVA; variations in energy output are automatically compensated to deliver the desired dose. With this system, the cells were exposed to accurate dosimetery of UVA radiation. On the basis of preliminary experiments cells were exposed to 4 J/cm^2 of UVA and harvested after 30 min (for ERK, STAT3, AKT1, mTOR, p70S6K, PCNA and Ki-67) or 24 h (for Bax, Bad, Bcl-X_L and DNA cell cycle), after which further studies were performed.

Preparation of total cell lysate. After treatment of cells with PFE or UVA (or both), the medium was aspirated and the cells were washed twice in PBS (10 m*M*, pH 7.4). The cells were incubated in 0.4 mL ice-cold lysis buffer (50 m*M* Tris-HCl, 150 m*M* NaCl, 1 m*M* ethyleneglycol-bis(aminoethylether)-tetraacetic acid [EGTA], 1 m*M* ethylene diaminetetraacetic acid [EDTA], 20 m*M* NaF, 100 m*M* Na_3VO_4, 0.5% Nonidet P-40 [NP-40], 1% Triton X-100 and 1 m*M* phenylmethylsulfonyl fluoride [pH 7.4]) with freshly added protease-inhibitor cocktail (Protease Inhibitor Cocktail Set III; Calbiochem, La Jolla, CA). The cells were then centrifuged at 13 000 ***g*** for 25 min at 4°C and the supernatant (total cell lysate) was collected, aliquoted and stored at –80°C.

Western blot analysis. For Western blot analysis, 25–30 μg of protein was resolved over 8–12% polyacrylamide gels and transferred to a nitrocellulose membrane. The blot containing the transferred protein was blocked in blocking buffer (5% nonfat dry milk, 1% Tween 20 in 20 m*M* Tris-buffered saline [pH 7.6]) for 1 h at room temperature followed by incubation with appropriate monoclonal primary antibody in blocking buffer for a duration ranging from 1 h to overnight at 4°C. This was followed by incubation with anti-mouse or anti-rabbit secondary antibody horseradish peroxidase for 1 h, several washings and detection by chemiluminescence (ECL kit, Amersham Life Sciences) and autoradiography using XAR-5 film obtained from Eastman Kodak Co. (Rochester, NY). Densitometric measurements of the band in Western blot analysis were performed using the digitalized scientific software program UN-SCAN-IT (Silk Scientific Corporation, Orem, UT).

Immunocytochemistry. NHEK were grown in two-chamber tissue-culture glass slides. At 70–80% confluence, cells were pretreated with PFE (as detailed earlier) and exposed to UVA (4 J cm^{-2}) and 30 min later cells were fixed in cold methanol (–20°C) for 10 min. Briefly, cells were incubated with TBST (50 m*M* Tris HCl, 150 m*M* NaCl and 0.1% Triton X-100 [pH 7.4]) for 10 min and then washed with TBS. Five percent goat serum in TBS (50 m*M* Tris HCl and 150 m*M* NaCl [pH 7.4]) was added to prevent nonspecific antibody binding. The cells were incubated with anti-human Ki-67 antibody (diluted to 1:50 in 10% goat serum) overnight at 4°C, followed by application of secondary anti-rabbit IgG antibody horseradish peroxidase conjugate for 1 h. Immunoreactions were visualized with DAB as substrate after counterstaining with eosin. Simultaneously, each slide was incubated with isotype control (IgG_1) as an internal negative control. Slides were

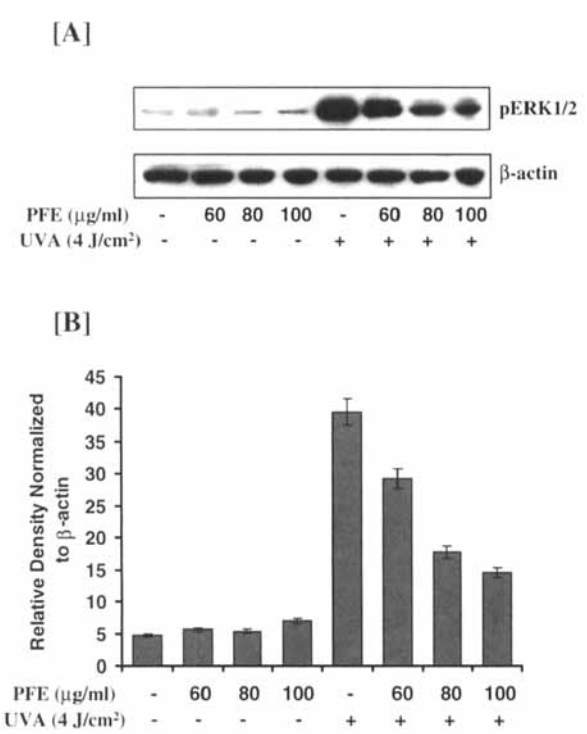

Figure 1. PFE treatment of NHEK inhibits UVA-mediated phosphorylation of ERK1/2. For dose-dependent studies NHEK were pretreated with PFE (60, 80 and 100 μg/mL) for 24 h after which the media was removed and cells were washed with PBS. Fresh PBS was added and cells were exposed to UVA (4 J cm^{-2}). Thirty minutes after the UVA dose, cells were harvested and total cell lysates were prepared for Western blot analysis, as detailed in Materials and Methods. (A) Protein levels of phosporlyated ERK1/2, determined by Western blot analysis. Equal loading was confirmed by stripping the blot and reprobing it for β-actin. The data shown here are from one representative experiment repeated three times with similar results. (B) Histogram representing the relative density of the Western blot bands normalized to β-actin. The quantification of protein was performed by densitometry analysis with UN-SCAN-IT software.

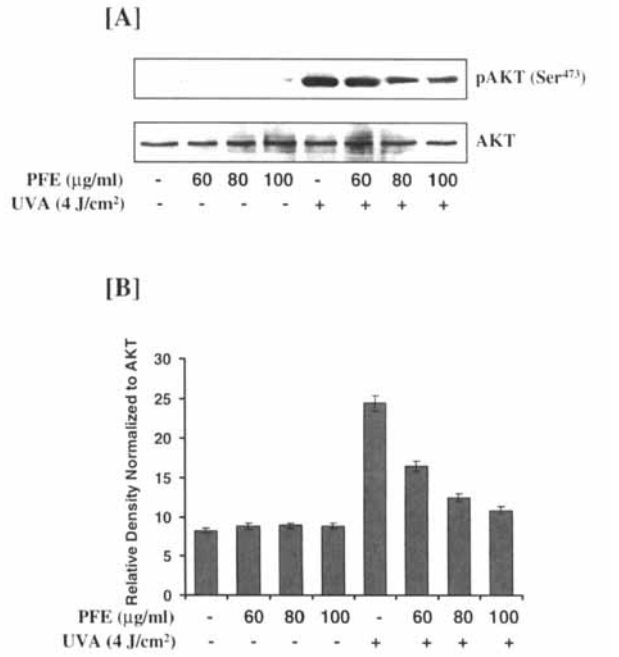

Figure 2. PFE treatment of NHEK inhibits UVA-mediated phosphorylation of AKT1 at Ser^{473}. For dose-dependent studies NHEK were pretreated with PFE and exposed to UVA (4 J cm^{-2}). Thirty minutes after the UVA dose, total cell lysates were prepared for Western blot analysis, as detailed in Materials and Methods. (A) Protein levels of phosphorylated AKT1, revealed by Western blot analysis. Equal loading was confirmed by stripping the blot and reprobing it for total AKT1. The data shown here are from one representative experiment repeated three times with similar results. (B) Histogram representing the relative density of the Western blot bands normalized to total AKT1. The quantification of protein was performed by densitometry analysis with UN-SCAN-IT software.

visualized on a Zeiss-Axiophot DM HT microscope. Images were captured with an attached camera linked to a computer. Images and figures were created by using ADOBE PHOTOSHOP 7.0 (Adobe Systems, Mountain View, CA).

DNA cell cycle analysis. NHEK (70–80% confluent) were treated with PFE (as detailed earlier) and after exposure to UVA (4 J cm^{-2}) cells were harvested in complete medium for 24 h. The cells were then trypsinized, washed with PBS and processed for labeling with fluorescein-tagged dUTP nucleotide and propidium iodide with the Apo-direct apoptosis kit (Phoenix Flow Systems) in accordance with the manufacturer's protocol. Labeled cells were analyzed by flow cytometry.

RESULTS

PFE treatment of NHEK inhibits UVA-mediated phosphorylation of ERK1/2

It has been shown that UVA exposure of keratinocytes results in the phosphorylation of ERK1/2 (13). To determine the effect of PFE on UVA-mediated phosphorylation of ERK1/2 in NHEK, Western blot analysis was performed using phosphospecific ERK1/2 antibodies. NHEK pretreated with PFE (60–100 μg/mL) were irradiated with 4 J cm^{-2} UVA, and 30 min after UVA irradiation cell lysate was prepared and Western blot analysis was performed. UVA exposure of NHEK resulted in marked phosphorylation of ERK1/2 (Fig. 1A). Western blot analysis and the relative density of bands revealed that, in PFE-pretreated cells, the extent of phosphorylation of ERK1/2 was found to decrease in a dose-dependent manner (Fig. 1A,B). A decrease in the phosphorylation of ERK1/2 was seen at 60 μg/mL with progressive inhibition at 100 μg/mL (Fig. 1A,B). These data demonstrate that ERK1/2 is phosphorylated by UVA exposure to NHEK and that PFE inhibits its phosphorylation in a dose-dependent manner.

PFE treatment of NHEK inhibits UVA-mediated phosphorylation of AKT1

Phosphorylation of AKT1 has recently been suggested as an additional step in the cascade of events leading to AKT1 activation. In this study, using an antibody that specifically recognizes AKT1 phosphorylated at Ser^{473}, we demonstrated that irradiation of NHEK with UVA (4 J cm^{-2}) resulted in phosphorylation of AKT1 at Ser^{473} 30 min after exposure (Fig. 2). As evident from Western blot analysis and the relative density of each band, we found that pretreatment of NHEK with PFE (60–100 μg/mL) for 24 h resulted in a dose-dependent inhibition of UVA-mediated phosphorylation of AKT1 at Ser^{473} (Fig. 2A,B).

PFE treatment of NHEK inhibits UVA-mediated phosphorylation of STAT3

Studies have shown that phosphorylation of STAT3 at Tyr^{705} is a prerequisite for its dimerization, DNA binding and transactivation, whereas phosphorylation at Ser^{727} alone does not

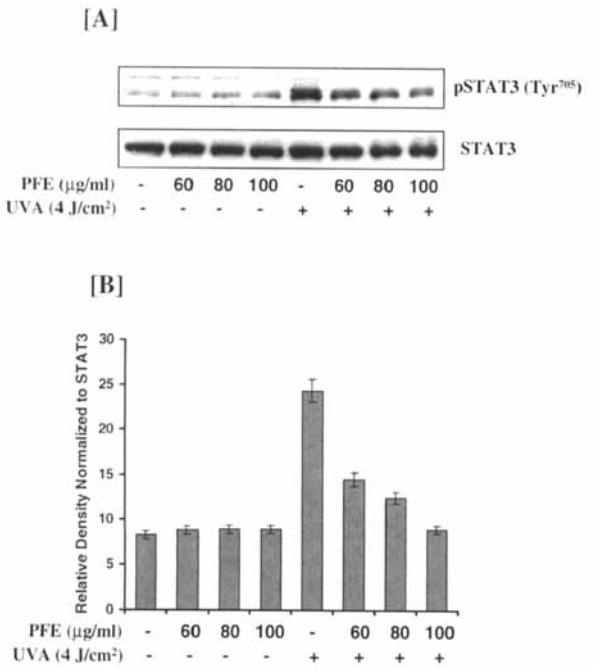

Figure 3. PFE treatment of NHEK inhibits UVA-mediated phosphorylation of STAT3 at Tyr^{705}. For dose-dependent studies NHEK were pretreated with PFE and exposed to UVA (4 J cm^{-2}). Thirty minutes after the UVA dose, total cell lysates were prepared for Western blot analysis, as detailed in Materials and Methods. (A) Protein levels of phosphorylated STAT3, revealed by Western blot analysis. Equal loading was confirmed by stripping the blot and reprobing it for total STAT3. The data shown here are from one representative experiment repeated three times with similar results. (B) Histogram representing the relative density of the Western blot bands normalized to total STAT3. The quantification of protein was performed by densitometry analysis with UN-SCAN-IT software.

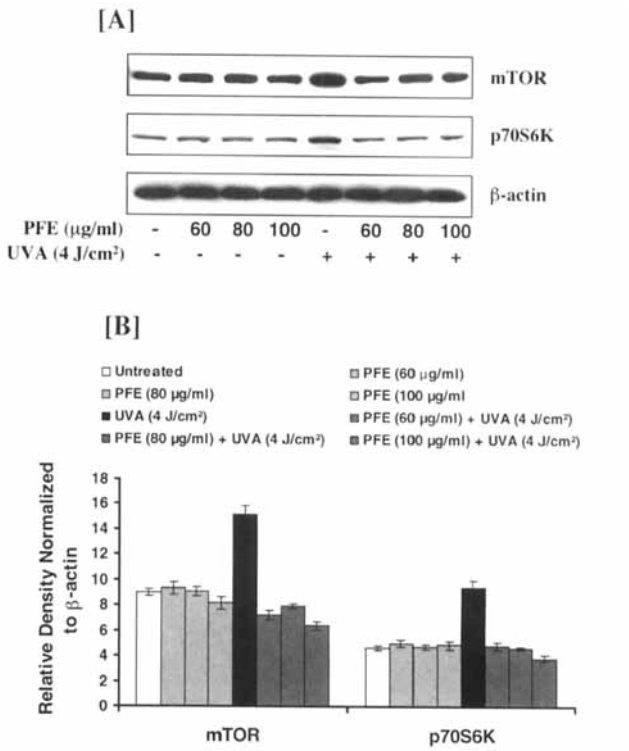

Figure 4. PFE treatment of NHEK inhibits UVA-mediated phosphorylation of mTOR and p70S6K. For dose-dependent studies NHEK were pretreated with PFE and cells were exposed to UVA (4 J cm^{-2}). Thirty minutes after the UVA dose, total cell lysates were prepared for Western blot analysis, as detailed in Materials and Methods. (A) Protein levels of phosphorylated mTOR and p70S6K, revealed by Western blot analysis. Equal loading was confirmed by stripping the Western blot and reprobing it for β-actin. The data shown here are from one representative experiment repeated three times with similar results. (B) Histogram representing the relative density of the Western blot bands normalized to β-actin. The quantification of protein was performed by densitometry analysis with UN-SCAN-IT software.

stimulate STAT3 DNA binding and transcriptional activities (25). In our studies UVA exposure of NHEK was found to result in phosphorylation of STAT3 at Tyr^{705} (Fig. 3), whereas no phosphorylation was evident at Ser^{727} at the dose selected (data not shown). Next we determined whether pretreatment of NHEK with PFE inhibited UVA-induced phosphorylation of STAT3 at Tyr^{705}. Western blot analysis and the relative density of bands revealed that pretreatment of NHEK with PFE resulted in a significant decrease in UVA-mediated activation of STAT3 in a dose-dependent manner (Fig. 3A,B).

PFE treatment of NHEK inhibits UVA-mediated phosphorylation of mTOR and its downstream target p70S6K

Studies have shown mTOR to be a direct upstream mediator of p70S6K, which is responsible for the phosphorylation 40S ribosomal protein S6 due to a number of extracellular stimuli (26). mTOR activity in turn may be affected by AKT1 through direct phosphorylation of the tuberous sclerosis tumor suppressor complex (27). The aim of this study was to investigate whether pretreatment of NHEK with PFE inhibits UVA-mediated phosphorylation of mTOR and its downstream target p70S6K. As evident from Western blot analysis, we found that UVA exposure to NHEK resulted in the phosphorylation of mTOR at Thr^{2448} and its downstream target p70S6K at Thr^{421}/Ser^{424} (Fig. 4A). Interestingly, we found that pretreatment of NHEK with PFE resulted in a significant downregulation of UVA-mediated phosphorylation of mTOR and its downstream target p70S6K (Fig. 4A,B). These data suggest that PFE restores cell growth to a controlled state by repressing the rate of protein synthesis.

PFE treatment of NHEK inhibits UVA-mediated increase in PCNA and Ki-67 protein expression

The proliferating cells that sustain UV-induced damage may continue cell division by using a damaged DNA template. PCNA is integral to nucleic acid synthesis and metabolism and its expression is notably increased in dividing cells. Immunoblot analysis revealed that UVA exposure to NHEK resulted in upregulation of PCNA, a marker of cell proliferation, and PFE pretreatment of these cells resulted in a dose-dependent decrease in the expression of the protein (Fig. 5A). Next we assessed the effect of PFE on UVA-mediated modulation of Ki-67, another marker of cell proliferation. As shown by immunocytochemical analysis, there was weak nuclear staining of Ki-67 in control and PFE-treated cells (Fig. 5B). In contrast, stronger Ki-67 staining was evident in NHEK 30 min after UVA exposure. Pretreatment with PFE resulted in marked reduction in the UVA-mediated increase of Ki-67 protein expression. Because Ki-67 is known to be expressed in the cells at all proliferative stages of the cell cycle (except the G_0 phase), our data demonstrate the antiproliferative potential of PFE.

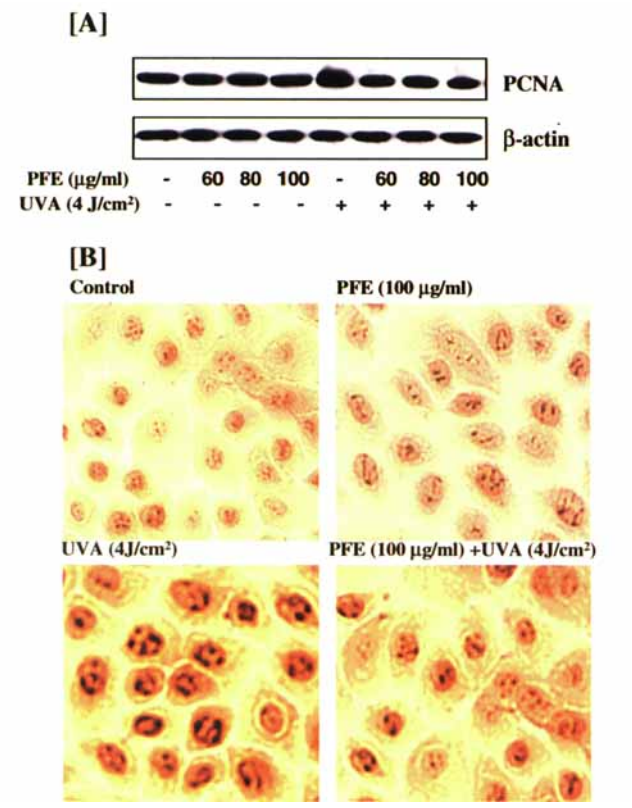

Figure 5. PFE treatment of NHEK inhibits UVA-mediated increase in markers of cell proliferation, as measured by PCNA and Ki-67 expression. (A) For dose-dependent studies NHEK were pretreated with PFE and exposed to UVA (4 J cm^{-2}). Thirty minutes after the UVA dose, total cell lysates were prepared as detailed in Materials and Methods, and Western blot analysis was performed to measure PCNA protein expression. Equal loading was confirmed by stripping the Western blot and reprobing it for β-actin. The data shown here are from one representative experiment repeated three times with similar results. (B) To determine Ki-67 staining patterns, NHEK were grown in tissue-culture slides, treated with PFE (100 μg/mL) for 24 h and exposed to UVA (4 J cm^{-2}). Thirty minutes after the UVA dose, the cells were stained for Ki-67, as detailed in Materials and Methods. A brown color indicates the presence of Ki-67 protein in the nuclei of cells. Counterstaining was performed with eosin (original magnification, ×400). The data shown here are from one representative experiment repeated two times with similar results.

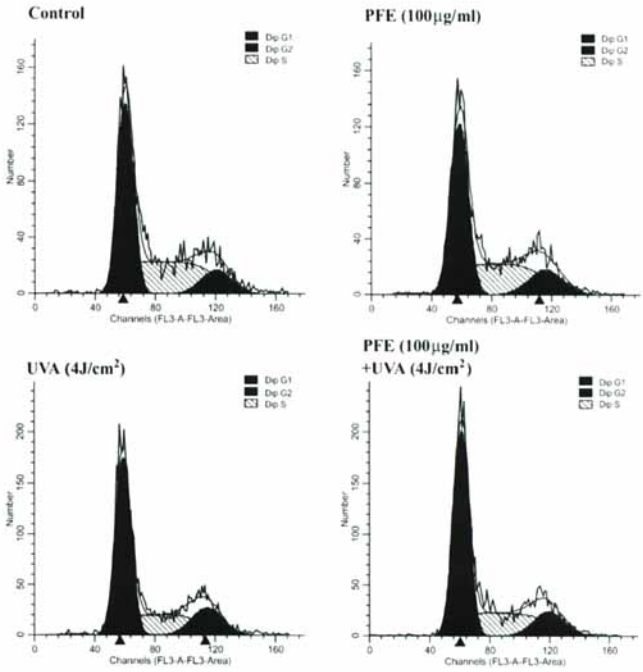

Figure 6. Effect of PFE treatment on cell-cycle distribution. For cell cycle studies NHEK were pretreated with PFE and exposed to UVA (4 J cm^{-2}). A total of 24 h after the UVA dose, cells were analyzed by flow cytometry as detailed in Materials and Methods. The percentage of cells in different phases of cell cycle was calculated using Modfit computer software. The data shown here are from a representative experiment repeated three times with similar results.

PFE treatment of NHEK results in augmentation of UVA-mediated cell cycle arrest

Studies have shown that the induction of apoptosis is cell-cycle dependent. Therefore, we performed DNA cell-cycle analysis to assess the effect of PFE treatment on UVA-mediated distribution of cells in the cell cycle. As shown in Fig. 6, there was an increase (57%) in the number of cells in G_1 phase of the cell cycle 24 h after UVA exposure, compared with the control cells (48%) and cells treated with PFE alone (49%). This effect was augmented by PFE treatment, with a 59% increase in the number of cells in G_1 phase.

Effect of PFE on UVA-mediated modulations in protein levels of Bcl-2 family

The expression of the antiapoptotic protein Bcl-X_L has been shown to be positively regulated by the transcription factor STAT3 in various cell lines (28). Because PFE treatment resulted in inhibition of phosphorylation of STAT3 at Tyr^{705}, we next assessed the effect of PFE on UVA-mediated modulations in Bcl_2 family members. It is well established that UV exposure results in the formation of apoptotic cells. Using Western blot analysis, we found that UVA exposure to NHEK resulted in upregulation of Bax and Bad, with a concomitant decrease in Bcl-X_L protein expression (Fig. 5A). We found that PFE treatment (60–100 μg/mL) further augmented UVA-induced decrease in Bcl-X_L, with a concomitant increase in Bax and Bad protein expression in a dose-dependent manner, as determined by Western blot analysis and the relative density of bands (Fig. 7A,B).

DISCUSSION

Although numerous studies have been conducted on the impact of UV radiation on skin cells, the beneficial effect of photochemopreventive agents on UVA-induced damage on human skin is less well-defined. UVA has been shown to be a potent inducer of various reactive oxygen species (primarily singlet oxygen), as well as a cause of lipid peroxidation in cell membranes (3). Antioxidant defense mechanisms may be overwhelmed by excessive free-radical generation, with resultant damage to the cells and increased chances of photocarcinogenesis. Studies in a mouse model have shown UVA to be a relatively weak initiator of carcinogenesis but a relatively potent tumor promoter (1). Development of new antioxidant strategies by supplementing the natural defense mechanism operating in the skin may be an important strategy in inhibiting UV-induced effects in the skin. Consistent with this hypothesis, there is an increasing trend of regular intake of dietary antioxidants or treatment of the skin with products containing antioxidant ingredients. Studies by us and others have shown that PFE and other naturally

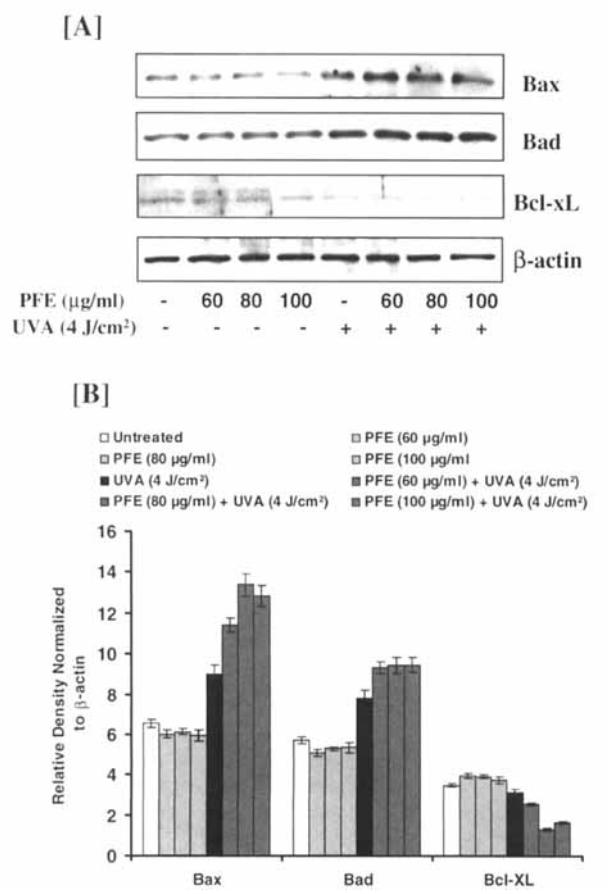

Figure 7. Effect of PFE on UVA-mediated modulations in levels of protein from the Bcl-2 family. For dose-dependent studies NHEK were pretreated with PFE and cells were exposed to UVA (4 J cm^{-2}). A total of 24 h after UVA, total cell lysates were prepared for Western blot analysis, as detailed in Materials and Methods. (A) Protein levels of Bax, Bad and Bcl-X_L, determined by Western blot analysis. Equal loading was confirmed by stripping the blot and reprobing it for β-actin. The data shown here are from one representative experiment repeated three times with similar results. (B) Histogram representing the relative density of the Western blot bands normalized to β-actin. The quantification of protein was performed by densitometry analysis with UN-SCAN-IT software.

occurring antioxidants, such as green tea, are effective in reducing the adverse effects of UVB-mediated cutaneous damage (1,6,29).

Pomegranate fruit extract (PFE), derived from the tree of *P. granatum*, is a rich source of two types of polyphenolic compounds—anthocyanins and hydrolyzable tannins—and possesses potent antioxidant and anti-inflammatory properties (21,22). Recently we have shown that topical application of PFE inhibited tumor development in a mouse skin model involving two-stage carcinogenesis (23). PFE inhibited gastric mucosal injury in animal models through its antioxidant activity (30), and in another study methanolic extract of dried pomegranate peel was shown to increase the rate of wound healing in rat skin (31).

The relevance of using UVA as a genotoxic agent and skin as the organ system of choice is based on the fact that UVA is a naturally occurring carcinogen for epidermal cells, the primary target of solar radiation. In our study NHEK were exposed to a UVA dose of 4 J cm^{-2}; this dose was selected on the basis of the observation that individuals with sensitive skin develop polymorphous light eruptions after a UV dose of as little as 5 J cm^{-2}. Interestingly, the same dose is known to cause rashes in patients who have chronic actinic dermatitis (32).

In this study we provide evidence of the photochemopreventive role of PFE by inhibition of UVA-mediated phosphorylation of ERK1/2, STAT3 and AKT1, with downregulation of PCNA and Ki-67 and a concomitant decrease of mTOR and p70S6K in NHEK. MAPK cascade, a three-kinase module conserved in all eukaryotes, has been shown to be activated in response to UVA in various cell lines (33). MAPK activation may result in proliferation by promoting AP-1 activation and subsequent upregulation of proto-oncogenes, such as cyclin D1 (34). Another study suggests that UVR-activated Ras-family proteins initially promote transient cell proliferation via ERK signaling, followed by cell cycle arrest *via* p38 (35). In the present study we found that UVA exposure to NHEK resulted in phosphorylation of ERK1/2 and that pretreatment of NHEK with PFE (60–100 μg/mL) for 24 h resulted in a dose-dependent inhibition of UVA-mediated phosphorylation of ERK1/2 (Fig. 1).

AKT1 activation may result in increased proliferation of the epidermal keratinocytes and the ability to resist terminal differentiation during multistage skin carcinogenesis. Also, mast cells with activated AKT1 may persist within the stroma of papillomas during skin tumor development, contributing to a pro-oxidant and proangiogenic microenvironment (36). Loss of PTEN function has been associated with AKT phosphorylation, cell growth and proliferation. Activation of AKT1 in response to UV-induced oxidant injury can influence cell survival by contributing to carcinogenesis. In this study we showed that NHEK exposure to UVA resulted in increased phosphorylation of AKT1 at Ser^{473} and that PFE treatment inhibits the phosphorylation in a dose-dependent manner (Fig. 2).

Abrogation of STAT3 function leads to apoptosis or inhibition of cell proliferation in various cancerous cell lines, including keratinocytes and papilloma cells, all of which harbor an activated gene encoding Ha-ras (37). Requirement of STAT3 in the development of skin tumors and maintenance of their autonomous growth has been shown and, more importantly, it was found that mice deficient in STAT3 were resistant to skin tumor development (38). It is well documented that STAT3 requires phosphorylation at tyrosine to undergo activation and translocation to the nucleus (39). Our data suggest that, following integration of signals from signaling molecules, including ERK and AKT1 induced concurrently by UVA stimulation, STAT3 was phosphorylated at Tyr^{705} whereas PFE pretreatment (60–100 μg/mL) of the cells resulted in a significant decrease in this phosphorylation in a dose-dependent manner (Fig. 3).

Because PFE has antiproliferative properties, we next investigated whether PFE can modulate UVA-induced mTOR and p70S6K expression. MAPK shares a consensus motif with the proline-directed Ser/Thr sites (Ser411, Ser418, Thr421 and Ser424) for p70S6K and has been shown to be involved in the phosphorylation and activation of p70S6K in response to UVA irradiation through H_2O_2 generation (40). UVA-mediated phosphorylation of mTOR and p70S6K may be responsible for an accelerated rate of protein synthesis and activation of tumor-cell proliferation. Rapamycin and its derivatives have been used to block mTOR functions and to yield antiproliferative activity in a variety of malignancies. Inhibition of mTOR with resultant G1-S cell-cycle delay and eventual apoptosis, as well as decreased phosphorylation of p70S6K, may be beneficial in the targeting of tumor cells. Immunoblot analysis showed that PFE (60–100 μg/mL) decreased the UVA-mediated phosphorylation of mTOR at Thr^{2448}, with concomitant downregulation of p70S6K at Thr^{421}/Ser^{424} (Fig. 4). The mTOR/p70S6K signaling cascade has been recognized to regulate UVB-induced DNA dam-

age and repair responsible for the enhanced synthesis of metalloproteinases, contributing to connective-tissue degradation in photoaging and to tumor progression (41). The current study provides evidence that this pathway is induced by UVA in NHEK and that PFE can be an effective agent in modulating this pathway, which may have implications for treatment of UVA-mediated damages.

If DNA damage induced by UV is not repaired, it may result in cell transformation, uncontrolled proliferation and, eventually, tumor formation on the skin (42). PCNA is synthesized in variable amounts by proliferating cells of both normal and transformed origin. There is considerable evidence that this ubiquitous and tightly regulated DNA-replication protein plays a major role in regulating the pathway(s) leading to DNA replication and cell division (43) and its expression has been used as a prognostic marker for tumor progression and metastasis. Insights into UV-induced proliferative pathways could help in modulating the propensity of cells to undergo apoptosis, either by enhancing the efficiency of cancer treatments or averting the unwanted death of normal cells. Ki-67, another important indicator of cell proliferation, contributes to the development of skin cancer through stimulation of cell division. Our data show that UV exposure to NHEK resulted in increased expression of PCNA and Ki-67 (Fig. 5A,B). Pretreatment with PFE resulted in decreased expression of these proliferative markers, suggesting that PFE is capable of providing protection against UVA-induced damage in epidermal keratinocytes by inhibiting cell proliferation.

AKT and other proliferative pathways deliver a survival signal in UV-treated cells. However, this appears to delay but not completely block UV-induced apoptosis in human keratinocytes. DNA damage caused by UV radiation initiates cellular-recovery mechanisms, which involve activation of DNA damage–response pathways. To assess the effect of PFE on cell division, we performed DNA cell-cycle analysis. A decrease in proliferation and an increased frequency of apoptosis are seen 24 h after doses of UVA irradiation (44). In accordance with these findings, our data show that NHEK exposure to UVA resulted in an increase in cell population in the G_1 phase of the cell cycle. PFE treatment was found to further augment this increase in cell population in the G_1 phase in NHEK (Fig. 6).

The processes of apoptosis and proliferation in response to UVR are closely linked and any dysregulation may lead to the development of skin cancer (45). Bcl-X_L exerts its antiapoptotic effect, at least in part, by binding to Bax and related proapoptotic proteins and also by preventing these proteins from inducing the release of cytochrome c and activating caspase-9. A direct link to the apoptosis-regulating proteins has been established through AKT phosphorylation of Bad (43,44). Inactivation of AKT prevents it from phosphorylating Bad at Ser^{136}. As a result, Bad becomes bound to Bcl-2, increasing its proapoptotic activity. Our results demonstrate that PFE treatment of NHEK resulted in increased expression of Bax and Bad with a corresponding decrease in Bcl-X_L expression, shifting the balance in favor of apoptosis (Fig. 7).

In conclusion, our data suggest that PFE has the potential to attenuate UVA-induced stress-mediated pathways associated with a high risk of carcinogenesis. This provides a molecular basis to conduct in-depth studies to determine the active components present in PFE that are responsible for its photochemopreventive effects.

Acknowledgement—This work was supported by a grant from the Lynda and Stewart Resnick Revocable Trust.

REFERENCES

1. Bowden, G. T. (2004) Prevention of non-melanoma skin cancer by targeting ultraviolet-B-light signalling. *Nat. Rev. Cancer* **4**, 23–35.
2. Harris, R. B. and D. S. Alberts (2004) Strategies for skin cancer prevention. *Int. J. Dermatol.* **43**, 243–251.
3. Bachelor, M. A. and G. T. Bowden (2004) UVA-mediated activation of signaling pathways involved in skin tumor promotion and progression. *Semin. Cancer Biol.* **14**, 131–138.
4. deGruijl, F. R. (2002) Photocarcinogenesis: UVA vs. UVB radiation. *Skin Pharmacol. Appl. Skin Physiol.* **15**, 316–320.
5. Wang, Y., D. Gao, D. P. Atencio, E. Perez, R. Saladi, J. Moore, D. Guevara, B. S. Rosenstein, M. Lebwohl and H. Wei (2005) Combined subcarcinogenic benzo[a]pyrene and UVA synergistically caused high tumor incidence and mutations in H-ras gene, but not p53, in SKH-1 hairless mouse skin. *Int. J. Cancer* **116**, 193–199.
6. Afaq, F., V. M. Adhami and H. Mukhtar (2005) Photochemoprevention of ultraviolet B signaling and photocarcinogenesis. *Mutat. Res.* **571**, 153–173.
7. Zhang, Y., Y. Y. Cho, B. L. Petersen, A. M. Bode, F. Zhu and Z. Dong (2003) Ataxia telangiectasia mutated proteins, MAPKs, and RSK2 are involved in the phosphorylation of STAT3. *J. Biol. Chem.* **278**, 12650–12659.
8. Lim, C. P. and X. Cao (1999) Serine phosphorylation and negative regulation of Stat3 by JNK. *J. Biol. Chem.* **274**, 31055–31061.
9. Levy, D. E. and J. E. Darnell Jr. (2002) Stats: transcriptional control and biological impact. *Nat. Rev. Mol. Cell Biol.* **3**, 651–662.
10. Shen, Y., G. Devgan, J. E. Darnell Jr. and J. F. Bromberg (2001) Constitutively activated Stat3 protects fibroblasts from serum withdrawal and UV-induced apoptosis and antagonizes the proapoptotic effects of activated Stat1. *Proc. Natl. Acad. Sci. U S A* **98**, 1543–1548.
11. Ibuki, Y. and R. Goto (2002) Antiapoptotic effects induced by different wavelengths of ultraviolet light. *Photochem. Photobiol.* **75**, 495–502.
12. Widmann, C., S. Gibson, M. B. Jarpe and G. L. Johnson (1999) Mitogen-activated protein kinase: conservation of a three-kinase module from yeast to human. *Physiol. Rev.* **79**, 143–180.
13. He, Y. Y., J. L. Huang and C. F. Chignell (2004) Delayed and sustained activation of extracellular signal-regulated kinase in human keratinocytes by UVA: implications in carcinogenesis. *J. Biol. Chem.* **279**, 53867–53874.
14. Brenneisen, P., J. Wenk, M. Wlaschek, T. Krieg and K. Scharffetter-Kochanek (2000) Activation of p70 ribosomal protein S6 kinase is an essential step in the DNA damage-dependent signaling pathway responsible for the ultraviolet B-mediated increase in interstitial collagenase (MMP-1) and stromelysin-1 (MMP-3) protein levels in human dermal fibroblasts. *J. Biol. Chem.* **275**, 4336–4344.
15. Stewart, M. J. and G. Thomas (1994) Mitogenesis and protein synthesis: a role for ribosomal protein S6 phosphorylation? *Bioessays* **16**, 809–815.
16. Melnikova, V. O. and H. N. Ananthaswamy (2005) Cellular and molecular events leading to the development of skin cancer. *Mutat. Res.* **571**, 91–106.
17. Cho, S. H., M. Delehedde, J. Rodriguez-Villanueva, S. Brisbay and T. J. McDonnell (2001) Bax gene disruption alters the epidermal response to ultraviolet irradiation and in vivo induced skin carcinogenesis. *Int. J. Mol. Med.* **7**, 235–241.
18. Krajewski, S., M. Krajewska, A. Shabaik, H. G. Wang, S. Irie, L. Fong and J. C. Reed (1994) Immunohistochemical analysis of *in vivo* patterns of Bcl-X expression. *Cancer Res.* **54**, 5501–5507.
19. Pena, J. C., C. M. Rudin and C. B. Thompson (1998) A Bcl-xL transgene promotes malignant conversion of chemically initiated skin papillomas. *Cancer Res.* **58**, 2111–2116.
20. Li, Y., L. S. Ooi, H. Wang, P. P. But and V. E. Ooi (2004) Antiviral activities of medicinal herbs traditionally used in southern mainland China. *Phytother. Res.* **18**, 718–722.
21. Kelawala, N. S. and L. Ananthanarayan (2004) Antioxidant activity of selected foodstuffs. *Int. J. Food Sci. Nutr.* **55**, 511–516.
22. Lansky, E. P., W. Jiang, H. Mo, L. Bravo, P. Froom, W. Yu, N. M. Harris, I. Neeman and M. J. Campbell (2005) Possible synergistic prostate cancer suppression by anatomically discrete pomegranate fractions. *Invest. New Drugs* **23**, 11–20.
23. Afaq, F., M. Saleem, C. G. Krueger, J. D. Reed and H. Mukhtar (2005) Anthocyanin- and hydrolyzable tannin-rich pomegranate fruit extract

modulates MAPK and NF-kappaB pathways and inhibits skin tumorigenesis in CD-1 mice. *Int. J. Cancer* **113**, 423–433.
24. Afaq, F., A. Malik, D. Syed, D. Maes, M. S. Matsui and H. Mukhtar (2005) Pomegranate fruit extract modulates UV-B–mediated phosphorylation of mitogen-activated protein kinases and activation of nuclear factor kappa B in normal human epidermal keratinocytes. *Photochem. Photobiol.* **81**, 38–45.
25. Akira, S., Y. Nishio, M. Inoue, X. J. Wang, S. Wei, T. Matsusaka, K. Yoshida, T. Sudo, M. Naruto and T. Kishimoto (1994) Molecular cloning of APRF, a novel IFN-stimulated gene factor 3 p91-related transcription factor involved in the gp130-mediated signaling pathway. *Cell* **77**, 63–71.
26. Dufner, A. and G. Thomas (1999) Ribosomal S6 kinase signaling and the control of translation. *Exp. Cell Res.* **253**, 100–109.
27. Roux, P. P., B. B. Ballif, R. Anjum, S. P. Gygi and J. Blenis (2004) Tumor-promoting phorbol esters and activated Ras inactivate the tuberous sclerosis tumor suppressor complex via p90 ribosomal S6 kinase. *Proc. Natl. Acad. Sci. U S A* **101**, 13489–13494.
28. Hsu, S. Y. and A. J. Hsueh (2001) Tissue specific Bcl2 protein in apoptosis ovarian paradigm. *Physiology Rev.* **80**, 593–614.
29. Afaq, F., V. M. Adhami, N. Ahmad and H. Mukhtar (2002) Botanical antioxidants for chemoprevention of photocarcinogenesis. *Front. Biosci.* **7**, d784–d792.
30. Ajaikumar, K. B., M. Asheef, B. H. Babu and J. Padikkala (2005) The inhibition of gastric mucosal injury by *Punica granatum* L. (pomegranate) methanolic extract. *J. Ethnopharmacol.* **96**, 171–176.
31. Murthy, K. N., V. K. Reddy, J. M. Veigas and U. D. Murthy (2004) Study on wound healing activity of *Punica granatum* peel. *J. Med. Food* **7**, 256–259.
32. Hampton, P. J., P. M. Farr, B. L. Diffey and J. J. Lloyd (2004) Implication for photosensitive patients of ultraviolet A exposure in vehicles. *Br. J. Dermatol.* **151**, 873–876.
33. Zykova, T. A., Y. Zhang, F. Zhu, A. M. Bode and Z. Dong (2005) The signal transduction networks required for phosphorylation of STAT1 at Ser727 in mouse epidermal JB6 cells in the UVB response and inhibitory mechanisms of tea polyphenols. *Carcinogenesis* **26**, 331–342.
34. Hildesheim, J. and A. J. Fornace Jr. (2004) The dark side of light: the damaging effects of UV rays and the protective efforts of MAP kinase signaling in the epidermis. *DNA Repair* **3**, 567–580.
35. Kulms, D. and T. Schwarz (2002) Molecular mechanisms involved in UV-induced apoptotic cell death. *Skin Pharmacol. Appl. Skin Physiol.* **15**, 342–347.
36. Affara, N. I., B. L. Schanbacher, M. J. Mihm, A. C. Cook, P. Pei, S. R. Mallery, C. S. Trempus, J. A. Bauer and F. M. Robertson (2004) Activated Akt-1 in specific cell populations during multi-stage skin carcinogenesis. *Anticancer Res.* **24**, 2773–2781.
37. Mora, L. B., R. Buettner, J. Seigne, J. Diaz, N. Ahmad, R. Garcia, T. Bowman, R. Falcone, R. Fairclough, A. Cantor, C. Muro-Cacho, S. Livingston, J. Karras, J. Pow-Sang and R. Jove (2002) Constitutive activation of Stat3 in human prostate tumors and cell lines: direct inhibition of Stat3 signaling induces apoptosis of prostate cancer cells. *Cancer Res.* **62**, 6659–6666.
38. Chan, K. S., S. Sano, K. Kiguchi, J. Anders, N. Komazawa, J. Takeda and J. DiGiovanni (2004) Disruption of Stat3 reveals a critical role in both the initiation and the promotion stages of epithelial carcinogenesis. *J. Clin. Invest.* **114**, 720–728.
39. Herrington, J., L. S. Smit, J. Schwartz and C. Carter-Su (2000) The role of STAT proteins in growth hormone signaling. *Oncogene* **19**, 2585–2597.
40. Zhang, Y., Z. Dong, M. Nomura, S. Zhong, N. Chen, A. M. Bode and Z. Dong (2001) Signal transduction pathways involved in phosphorylation and activation of p70S6K following exposure to UVA irradiation. *J. Biol. Chem.* **276**, 20 913–20 923.
41. Brenneisen, P., J. Wenk, M. Wlaschek, T. Krieg and K. Scharffetter-Kochanek (2000) Activation of p70 ribosomal protein S6 kinase is an essential step in the DNA damage-dependent signaling pathway responsible for the ultraviolet B–mediated increase in interstitial collagenase (MMP-1) and stromelysin-1 (MMP-3) protein levels in human dermal fibroblasts. *J. Biol. Chem.* **275**, 4336–4344.
42. Erb, P., J. Ji, M. Wernli, E. Kump, A. Glaser and S. A. Buchner (2005) Role of apoptosis in basal cell and squamous cell carcinoma formation. *Immunol. Lett.* **100**, 68–72.
43. Celis, J. E., P. Madsen, A. Celis, H. V. Nielsen and B. Gesser (1987) Cyclin (PCNA, auxiliary protein of DNA polymerase delta) is a central component of the pathway(s) leading to DNA replication and cell division. *FEBS Lett.* **220**, 1–7.
44. Larsson, P., E. Andersson, U. Johansson, K. Ollinger and I. Rosdahl (2005) Ultraviolet A and B affect human melanocytes and keratinocytes differently. A study of oxidative alterations and apoptosis. *Exp. Dermatol.* **14**, 117–123.
45. Ouhtit, A., H. K. Muller, D. W. Davis, S. E. Ullrich, D. McConkey and H. N. Ananthaswamy (2000) Temporal events in skin injury and the early adaptive responses in ultraviolet-irradiated mouse skin. *Am. J. Pathol.* **156**, 201–207.
46. Nguyen, T. T., E. Tran, C. K. Ong, S. K. Lee, P. T. Do, T. T. Huynh, T. H. Nguyen, J. J. Lee, Y. Tan, C. S. Ong and H. Huynh (2003) Kaempferol-induced growth inhibition and apoptosis in A549 lung cancer cells is mediated by activation of MEK-MAPK. *J. Cell Physiol.* **197**, 110–121.
47. Chung, J. H., J. H. Han, E. J. Hwang, J. Y. Seo, K. H. Cho, K. H. Kim, J. I. Youn and H. C. Eun (2003) Dual mechanisms of green tea extract (EGCG)–induced cell survival in human epidermal keratinocytes. *FASEB J.* **17**, 1913–1915.